Concept of Secondary Heterogeneous Structure of Long-Chain Branched Polyethylene

TOKIO FUJIKI, *Polymer Laboratory, Nippon Polychemicals Co., Ltd. Nanyo-cho, Yamaguchi-ken, Japan*

Synopsis

The mechanism of formation of surface roughness and extrusion swelling of the extrudate and the steady-shear viscous flow behavior in the region of high shear rate for branched polymers were investigated using two low-density polyethylenes and their sheared samples. These two polyethylenes varied in their degree of branching, molecular weight, and molecular weight distribution but were similar in their melt flow index. The effect of molecular parameters, especially long-chain branching, on viscoelastic properties in the molten state was also considered. Samples of various degree of shearing level were prepared by passing them repeatedly through an extruder. Results of intrinsic viscometry, gel permeation chromatography, and infrared spectroscopy of the original and the sheared samples indicate that no appreciable variation between them takes place in the molecular parameters during the process of extrusion shearing. Both surface roughness and extrusion swelling of the extrudate diminish with increase in the extent of shear. The extrusion shearing affects the surface roughness and extrusion swelling of the extrudate as well as the capillary entrance effect more markedly for the highly branched polymers with considerably higher molecular weight than for the less branched species with bell-type molecular weight distribution. These results demonstrate that heterogeneity becomes more conspicuous with the degree of long-chain branching level, and therefore the role of long-chain branching in the development of the heterogeneity is particularly important. It is suggested that the secondary heterogeneous structure arises through phase separation or from the heterogeneous formation of strongly entangled network at the branching point of the long-chain branching in the manufacturing process of the low-density polyethylene and that its presence causes the distinctive viscoelastic properties of long-chain branched polymer melts.

INTRODUCTION

Branched polymers significantly differ from linear polymers in viscoelastic properties in the molten state, such as melt extensibility, temperature and molecular weight dependence of melt viscosity, surface roughness of the extrudate, etc. Structural studies[1-10] on rheological properties of branched polymer melts indicate that the characteristic features of the viscoelastic properties of branched polymer melts can be attributed especially to the presence of long-chain branching which arises from the chain transfer reaction to other polymers in the free-radical polymerization process.

The characteristics of a branched molecule, i.e., its dimensions, its flexibility, its segmental distribution, etc., have been investigated in detail theoretically or experimentally by many investigators through light-

47

scattering or intrinsic viscosity studies of branched polymers,[11] whereas the role of long-chain branching in causing the distinctive viscoelastic properties of branched polymer melts, in which molecules have certain intermolecular interactions, is not clear enough.

As is well known, the properties of dilute polymer solutions primarily reflect two kinds of intermolecular energetic interaction, called long-range interaction and short-range interaction. But at higher temperatures, where thermal molecular motions free themselves from the restraint of energetic interactions, certain stronger intermolecular interactions, such as intermolecular entanglement rather than energetic interactions, may be of special significance in causing the distinctive viscoelastic properties of branched polymer melts in relation to molecular structures, especially long-chain branching.

Recently, a very interesting study on anomalous melt flow properties for long-chain branched acetal polymers has been reported by Prichard and Wissbrun.[10] Increased melt flow rate of long-chain branched acetal polymers is achieved by continuous shearing; on the other hand, the dissolving and reprecipitating treatments of the sheared polymers lessen the increased melt flow rate. A change in melt flow rate by shearing or by dissolving and reprecipitating the sheared samples is pronounced in the crystalline branched polymers but is absent in linear or noncrystalline branched polymers. Accordingly, they attribute the reversibility of the melt flow rate for long-chain branched acetal polymers to the fact that the intermolecular chain entanglement, once disrupted by shearing, is reformed particularly at the branching point as the polymer is crystallized from the solution. Similar results have been reported for low-density polyethylene by Howells and Benbow[12] prior to these of Prichard and Wissbrun.[10] The reversal, in this case, was achieved by holding the sheared melt at 190°C for several hours.

The phenomena observed in these studies demonstrate a characteristic feature of the rheological properties of branched polymers in the molten state and clearly demonstrate a singularity of the intermolecular chain entanglement of branched polymers. If the rheological properties of the branched polymer are controlled by a strongly entangled network at the branching point, it is expected that shearing lessens melt viscosity when the entanglement is disrupted by shearing, because the entanglement possibly increases the flow resistance at the branching point, as suggested by Long and co-workers[4] for long-chain branched poly(vinyl acetate). Prichard and Wissbrun's results, however, indicate that shearing affects markedly elastic properties, such as entrance corrections for capillary and extrusion swelling of the extrudate, but does not affect melt viscosity.

McCord and Maxwell[13] suggested, as a conclusion of a study on the temperature dependence of elastic recovery for branched and linear polyolefins, that the elastic properties of the branched polyolefins are principally governed by intermeshing of side chain branches. Also, Nagasawa and Fujimoto[14] attempted to explain theoretically the molecular dependence

of melt viscosity for long-chain branched polystyrene of comb shape on the basis of interbranching entanglement.

We can see from these arguments that intermolecular entanglement, in some cases, appears to form at the branching point and, in other cases, it seems to be characterized by the intermeshing of chain branches. For this there are two possible explanations. One is possibly derived from the diversity of the branching structure—length and shape of branching and number of branching. The other may be ascribed to the fact that the state of the intermolecular entanglement is easily varied by mechanical stimulations such as shearing, as reported by Howells and Benbow[12] and Prichard and Wissbrun.[10] Especially in the latter case, since it is presumed that shearing markedly affects the rheological properties of branched polymer melts without change in the molecular structure, special attention should be paid to the shear history of the polymer in a structural study on the viscoelastic properties of the melt.

Studied in the present paper are the effect of shearing on surface roughness and extrusion swelling of the extrudate, and on the steady-shear viscous flow behavior in the region of high shear rate, using low-density polyethylenes of two kinds which differ in their degree of branching, molecular weight, and molecular weight distribution but are similar in their melt flow index. The effect of molecular parameters, especially long-chain branching, on viscoelastic properties in the molten state is also considered.

EXPERIMENTAL

Materials

Two kinds of the low-density polyethylene, H and L, produced by high-pressure process were used in this study. The resin characteristics—melt flow index (ASTM D1238-65T, procedure A) and density (ASTM D1505-63T) are 1.1 g/10 min and 0.917 g/ml, respectively, for sample H and 1.4 and 0.924, respectively, for sample L.

Since commercial low-density polyethylenes are kneaded in the molten state by intensive mixer for the addition of various additives, such as slip and anti-block agents, and pass repeatedly through the extruder for pelletization, they have in general a largely different shear history. For the purpose of this study, samples with a minimum shear history were prepared by diminishing the processes for commercialization.

The degree of long-chain branching was estimated from intrinsic viscosity measurements of fractions at the θ-temperature over a broad range of molecular weight with the above two samples and with Sholex 6050, a Marlex 50-type linear polyethylene. As is well known, the intrinsic viscosity of a highly branched polymer is lower than that of a less branched one of the same molecular weight. This reduced intrinsic viscosity of the branched polymer is basically ascribed to the small radius of gyration of a branched molecule in comparison with that of a linear molecule of the same molecular weight when dissolved in the same solvent. The number of long-
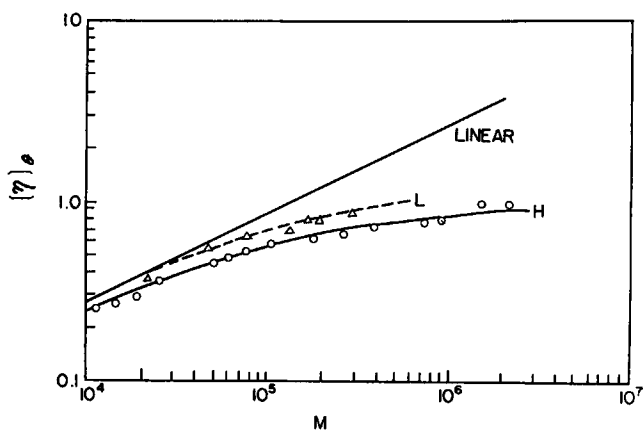
Fig. 1. Intrinsic viscosities vs. molecular weight plots for linear and two branched poly-
ethylenes, L and H, in dodecanol-1, at 138°C.

chain branching of the fractions, therefore, can be calculated from the
intrinsic viscosity of the branched and linear fractions.   However, in this
study, as the long-chain branching level of the whole polymer should be
taken into account, we do not deliberately calculate the number of long-
chain branching of the fractions.

Figure 1 represents the relationship between molecular weights and
intrinsic viscosities of the fractions of the two samples and of linear poly-
ethylene (Sholex 6050), which fractions were obtained by means of a
column elution fractionation technique in dodecanol-1 at 138°C of the θ-
temperature.   It is evident from Figure 1 that both polymers, H and L,
have considerable long-chain branches at higher molecular weights, but the
long-chain level of sample L is lower than that of sample H.

The samples exhibiting various degrees of shearing level were prepared
by passing from one to five times through a 40-mm extruder with a poly-
ethylene-type screw.   The extrusions were carried out under constant
resin pressure and temperature.   The extrusion conditions and extrusion
speed of the sheared samples, in g/min, are shown in Table I.

If variations occur in molecular weight, in molecular weight distribution,
and in the number of branching during the process of extrusion shearing,
then it will become very difficult to attribute the change in viscoelastic
properties of the melts to either the polymer structure or to other factors,
for example, the state of a certain intermolecular attachment due to the
extrusion shearing.   So, for the purpose of this study, no change should be
required in the polymer structure during the process of extrusion shearing.

The results of gel permeation chromatography, intrinsic viscometry, and
infrared-spectroscopic analysis both for the sheared samples and for the
nonprocessed original samples confirmed that there occurs no appreciable
change in molecular structure, i.e., molecular weight, molecular weight dis-
tribution, and endgroups in methyl groups per 1000 carbon atoms during
the process of extrusion shearing.   These results are numerically shown in

TABLE I

Processing Conditions of the Extrusion Shearing and Change of the
Extrusion Speed and Melt Flow Index

| Sample | Pass fre-quency | Temp., °C | | | Resin press.[c] kg/cm² | Screw speed, rpm | Ex-trusion speed, g/min | Melt index |
		C_1[a]	C_2[b]	Die				
	0	—	—	—	—	—	—	1.35
	1	121	165	160	100	49	159	1.37
L	2	123	165	160	100	54	176	1.38
	3	124	165	160	100	55	187	1.41
	4	124	165	160	100	55	187	—
	5	125	165	160	100	55	185	1.43
	0	—	—	—	—	—	—	1.05
	1	125	175	160	104	35	122	1.14
	2	125	174	160	104	44	153	1.24
H	3	125	174	160	104	52	180	1.27
	4	125	173	160	104	60	217	—
	5	125	173	160	104	60	221	1.32

[a] Cylinder No. 1.
[b] Cylinder No. 2.
[c] Screen pack, 80/100/80 mesh.

Table II, where molecular weights of the original and sheared samples are described in terms of both the number- and weight-average extended chain length obtained from the GPC elution curves, using plots of elution volume versus extended chain length of the polystyrene standards supplied by Pressure Chemical Company. The instrument, with a four-column Styragel combination of 10^3, 10^4, 10^5, and 10^6 angstroms, was operated at 135°C; 1,2,4-trichlorobenzene was used as the eluent solvent, and the eluent flow rate was 1 ml/min.

Figures 2 and 3 show typical normalized GPC elution curves, Figure 4 shows plots of η_{sp}/C versus concentration C in Tetralin at 135°C for two original samples, H-0 and L-0, and two sheared samples, H-5 and L-5.

TABLE II

Extended Chain Length and Methyl Group Content of Original and Sheared Samples

Sample	$\bar{A}_n$,[a] Å	$\bar{A}_w$,[b] Å	$\bar{A}_w/\bar{A}_n$	$CH_3/1000$ C
L-0	1270	3970	3.1	24
L-1	1270	3870	3.1	23
L-2	1170	3820	3.3	24
L-3	1290	3780	2.9	24
L-5	1240	4070	3.3	25
H-0	1920	18400	9.6	34
H-1	2060	18400	8.9	35
H-2	2030	17600	8.7	34
H-3	1980	18800	9.5	34
H-5	2240	19000	8.5	35

[a] Number-average extended chain length obtained from GPC data.
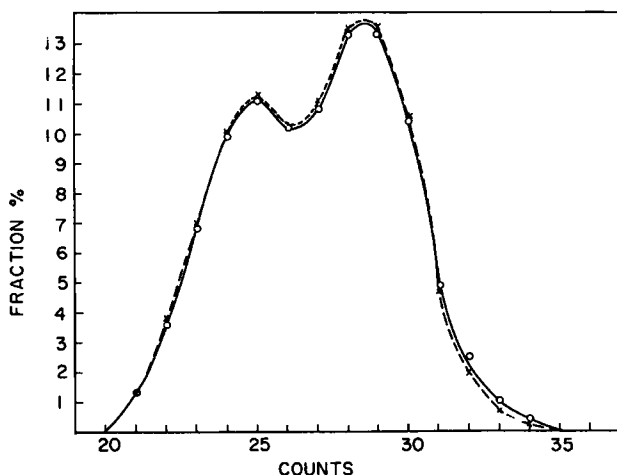[b] Weight-average extended chain length obtained from GPC data.

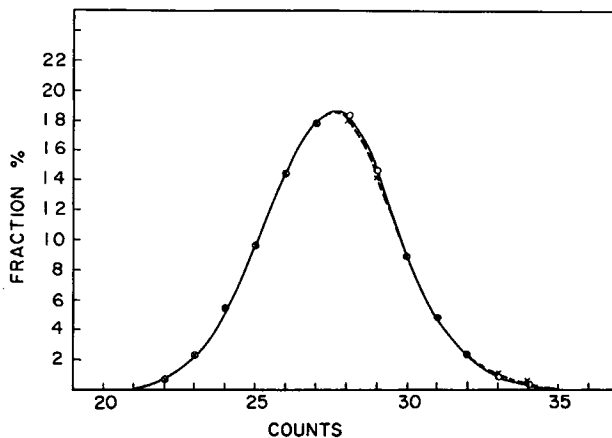Fig. 2. Normalized GPC elution curves for H-0 (—○—) and H-5 (— —×— —).

Fig. 3. Normalized GPC elution curves for L-0 (—○—) and L-5 (— —×— —).

(Here, the figure after the hyphen designates the pass frequency of the samples through the extruder.)   We can see from Table II and Figures 2 and 3 that sample H has a broader molecular weight distribution at the higher molecular side, in contrast to a bell-type molecular weight distribution of sample L.   Taking into account that GPC separation shows higher sensitivity to the presence of long-chain branching,[15] we can also see that no appreciable change in the number of short- and long-chain branchings occurs during the process of extrusion shearing within the limits of the experimental errors.

Also, in order to see if the samples have insoluble material or not, the original and sheared samples were extracted with xylene for 24 hr using a Soxhlet extractor.   The results of this experiment show that all the samples used in this study completely dissolve in hot xylene.
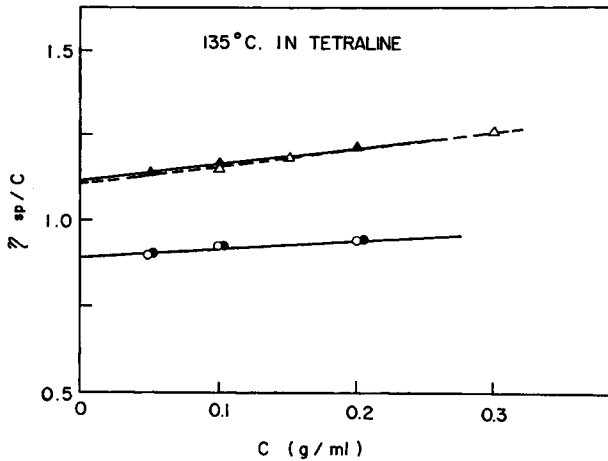
Fig. 4. η_{sp}/C ratios vs. concentration plots for H-0 ($\triangle$), H-5, ($\blacktriangle$) L-0 (O) and L-5 ($\bullet$) in Tetralin at 135°C.

Melt Viscosity

The melt viscosities in the region of high shear rate were measured at 190°C with a capillary-type rheometer Koka Flow Tester with flat dies of length-to-radius ratios (L/R) of 10, 20, and 30. For details of the operation of this rheometer, Arai's book[16] should be referred to.

Surface Roughness of the Extrudate

Since it is difficult to measure quantitatively the surface roughness of extrudates, it was numerically represented in this paper in terms of the external haze of the carefully blown film, which can be optically measured.

All the blown film extrusions were carried out under the same processing conditions using a 40-mm extruder with a polyethylene-type screw, with a screen combination of 80, 100, and 80 mesh and with a spider die 75 mm in diameter. The processing temperatures were 120°C in cylinder No. 1, and 165°C in cylinder No. 2 and in the die; the blow-up ratio was 2.12. All the blown films obtained was 38 microns in thickness.

The haze of low-density polyethylene film generally observed is the sum of the internal and external hazes. The former is mainly ascribed to light scattering by the crystalline granules and the latter, to the surface roughness of the extrusion film. The external haze (total haze minus internal haze), therefore, is directly proportional to the degree of surface roughness of the extrudate. Here, the haze of the film was measured according to ASTM designation D1003, Standard Method of Test for Haze and Laminous Transmittance of Transparent Plastics.

The internal haze can also be measured by the following procedure: silicon oil is uniformly smeared on both sides of a film sample of suitable size, and the film is put between two glass slides for microscopic use. The oil used is KF54, manufactured by Shinetsu Chemical Company, a material

having a viscosity of 400 centistokes at 25°C and a refractive index of 1.50–1.51 at 25°C. In the sample thus prepared, the light scattering due to film surface roughness vanishes because the surface is rendered smooth by the silicon oil, and the refractive index of the silicon oil is nearly equal to that of polyethylene.[17] The internal haze of the film was obtained from this sandwiched specimen according to ASTM D1003.

Extrusion Swelling

The extrusion in this study was carried out with a 30-mm extruder, manufactured by Brabender Corporation, having a die with a length-to-diameter ratio of 20:1. In order to avoid confusion arising from differences in shear rates, special attention was paid to keeping the extrusion speed constant for all samples. Extrusion conditions were: 150°C resin temperature and 145 rpm screw speed. Extrusion speed was 61.2 to 63.8 g/min for all samples, so the average rate of shear in the capillary must have been constant. Here, the swelling index, a measure of the degree of extrusion swelling, was defined as the ratio of the diameter of the extruded rod to that of the capillary.

RESULTS

As is seen from Table I, both the melt flow indices and the extrusion speeds, in g/sec, gradually increase with increase in shearing level, but rate of increase is greater in sample H, a highly long-chain branched polymer with considerably higher molecular weight species, than in sample L, a less long-chain branched polymer with a bell-type molecular weight distribution
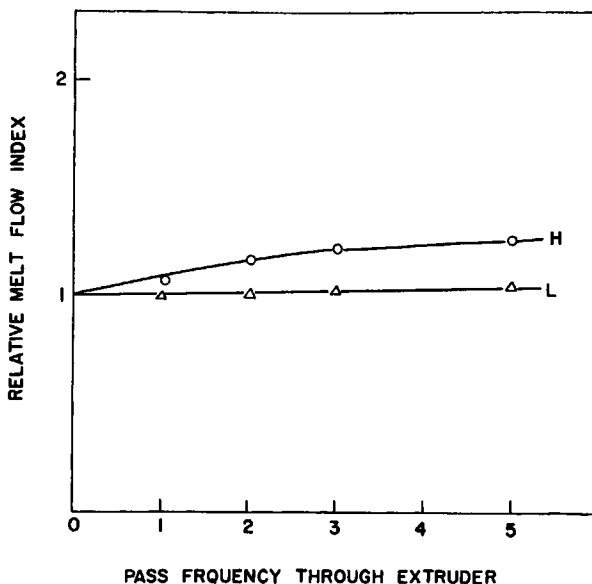

PASS FREQUENCY THROUGH EXTRUDER

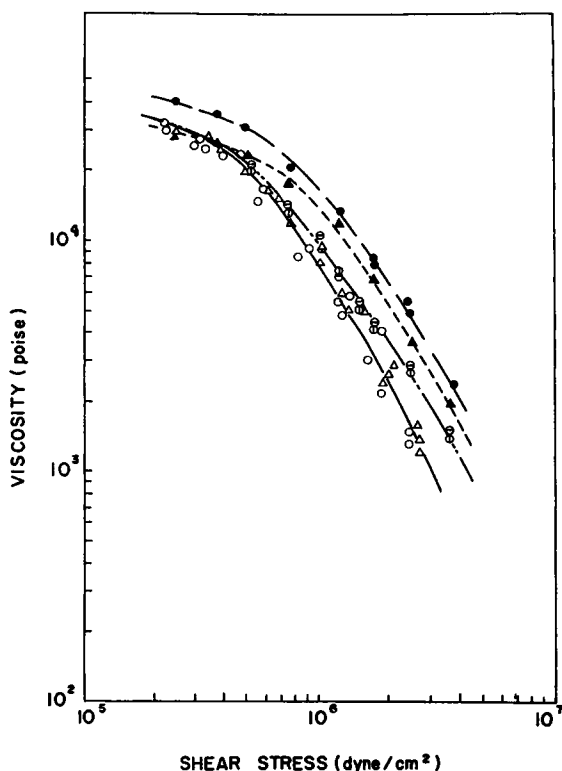Fig. 5. Effect of extrusion shearing on melt flow index.

Fig. 6. Shear stress dependencies of melt viscosity at 190°C for H-0 (● before; ○ after) and H-5, before and after capillary end corrections, (▲ before, △ after) and for L-0,(⊖) and L-5(⊕) before corrections. Curves before corrections were obtained using flat die of L/R ratio of 20.

Figure 5 shows the effect of the shear history, represented in terms of pass frequency through the extruder, on the melt flow indices for both samples H and L. As causes for the increased flow rate arising from passing of the polymers through the extruder, in general, two reasonable explanations will be given: (1) a lowering in melt viscosity during the process of extrusion shearing and/or (2) a decrease in the elastic responsivity of the melt which possibly results in lowering of the capillary end effects. The former is often observed in mastication of the rubbery materials, but we have scruples about accepting this explanation here, because no appreciable variation in the polymer structures occurs during the processing of the polymers.

Second, we will experimentally follow up an inquiry about the possibility of explanation (2). Figure 6 shows the relationship between shear stresses and melt viscosities at 190°C for the original samples H-0 and L-0 and the sheared samples H-5 and L-5. This figure indicates that there is scarcely any difference in the values of the melt viscosity of samples L-0 and L-5 and in their shear stress dependence, whereas there is a distinct differ-
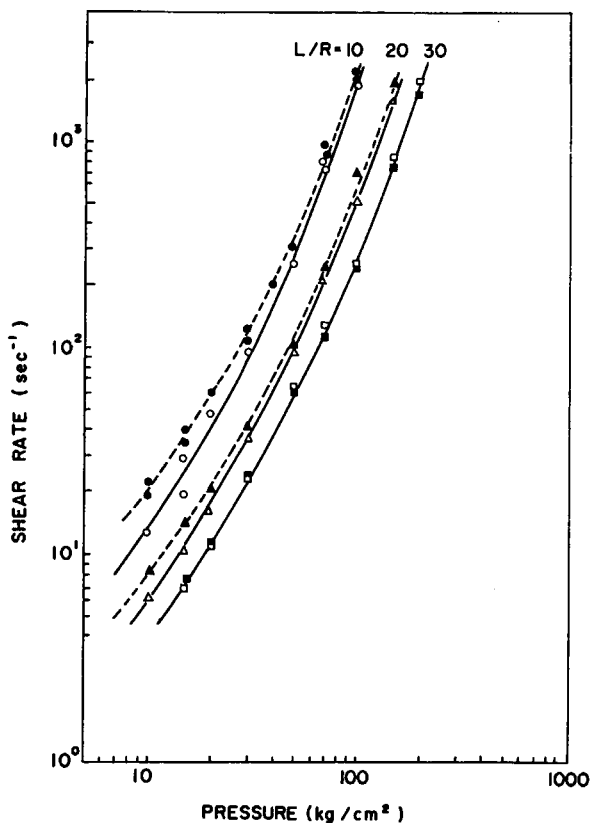
Fig. 7. Shear rate vs. applied pressure plots for H-0 (solid lines) and H-5 (dashed lines) at 190°C.

ence in those of samples H-0 and H-5 before the capillary end corrections are made. This result entirely shows the same tendency, as either melt flow index and/or extrusion speed depend on the shearing given to these samples.

If the change in the melt viscosity or in the melt flow rate, which is marked in the highly branched sample H, occurs mainly because of lowering of the capillary end effect due to the shear processing, then it is expected that the longer the length of the die capillary, the smaller the capillary end effect on the melt flow rate. Figure 7 clearly demonstrates the propriety of this expectation. In this figure the dotted curves represent the relationship between logarithm of the applied pressure and of the shear rate for sample H-5, and the solid curves, for sample H-0. The shear rate of sample H-5 is higher than that of the original, H-0, if comparison is made at the same applied pressure. However, the difference in the shear rate perceived between the original and sheared samples actually diminishes in proportion to the length of the capillary, that is, in the order 5 mm in length($L/R = 10$), 10 mm ($L/R = 20$), and 15 mm ($L/R = 30$). This finding is also demonstrated in the comparison of the values of the capillary end correction
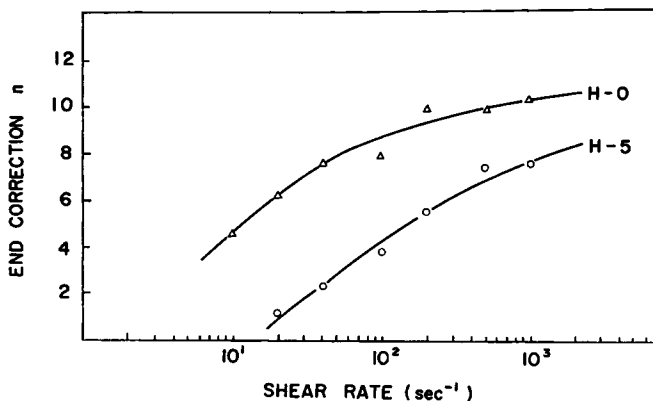
Fig. 8. Capillary and correction vs. shear rate for H-0 and H-5 at 190°C.

of sample H-0 with those of sample H-5, which were obtained by Bagley's method[18] and are indicated in Figure 8. It is clear from this figure that the higher shear rate of sample H-5 is based on the lower values of the capillary end correction. This result is in reasonable agreement with that of Prichard and Wissbrun[10] for long-chain branched acetal polymers and demonstrates also that the capillary end effect on the melt flow behavior of the highly long-chain branched polymer can not be ignored when the polymer has a shear history.

Figure 6 also compares the logarithmic plots of the apparent melt viscosities versus effective shear stresses for samples H-0 and H-5 before and after the capillary end corrections are made. We can see from Figure 6 that there is no difference in the corrected melt viscosities of both samples H-0 and H-5, being independent of the L/R ratio of the die used.

It is, therefore, concluded that the increase in the melt flow index or the decrease in the melt viscosity of the sheared samples is ascribed to the increase in the effective applied pressure, viz., to lowering of the values of the capillary end correction due to passing of the polymers through the extruder, rather than the variation in the polymer structure such as molecular weight, molecular weight distribution, etc.

As described above, the haze we generally observe of the extrusion film of the low-density polyethylenes consists of internal and external hazes. The latter possibly arises from two causes: the occurrence of melt fracture and of surface roughness. Many studies[19-24] on the formation of melt fracture indicate that it occurs at and above a critical shear stress according to a certain regular way in the formation of fracture, whereas the surface roughness found in the extrusion film or the extruded rod of the low-density polyethylene forms even at comparatively lower shear rates, and it also has no clear critical shear stress for its formation. One of the most significant characteristics of the surface roughness is in that when the extrudate is quenched by stretching it in the molten state, the surface roughness is markedly reduced (the commercial significance of the water quench-

TABLE III
Effect of Extrusion Shearing on Optical Properties of Blown Film

| Sample | Total haze, % | | Internal haze, % | | External haze, % | | Gloss, % | |
	Measured	Ratio	Measured	Ratio	Measured	Ratio	Measured	Ratio
L-0	3.4	1.00	0.80	1.00	2.60	1.00	12.3	1.00
L-1	3.3	0.97	0.71	0.89	2.59	1.00	12.3	1.00
L-2	3.2	0.94	0.67	0.84	2.53	0.97	12.7	1.03
L-3	2.7	0.79	0.63	0.79	2.07	0.80	12.6	1.02
L-5	2.5	0.74	0.63	0.79	1.87	0.72	12.8	1.04
H-0	16.0	1.00	0.74	1.00	15.3	1.00	6.5	1.00
H-1	12.9	0.81	0.59	0.80	12.3	0.81	7.6	1.17
H-2	9.7	0.61	0.50	0.68	9.20	0.60	8.5	1.31
H-3	7.6	0.48	0.48	0.65	7.12	0.47	9.4	1.45
H-5	5.2	0.33	0.45	0.61	4.75	0.31	10.6	1.63

ing applied for the blown film of the low-density polyethylene lies in an improvement in its optical properties). However, neither the mechanism of the formation of the surface roughness nor the relationship of it to the polymer structure is clear enough as yet. Table III shows values of the total, external, and internal hazes and of the gloss for the original and sheared ones of the above two samples and also their relative values, indicating the ratio of the value of the sheared one to that of the original one.
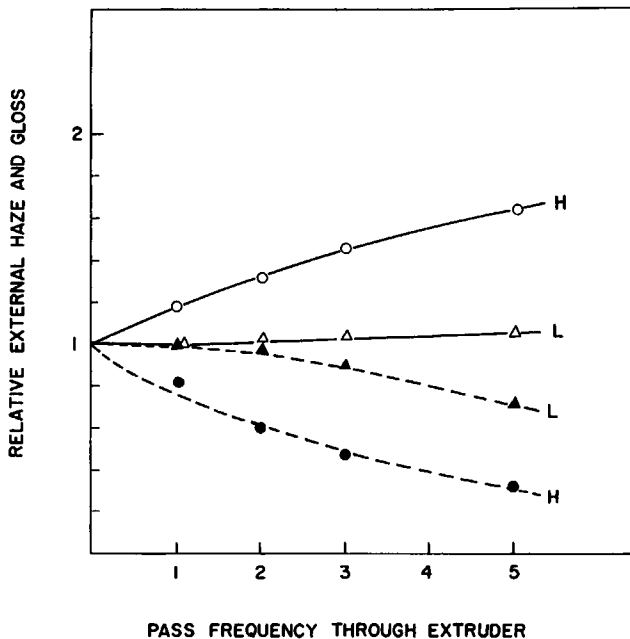

Fig. 9. Effect of extrusion shearing on external haze (dashed lines) and gloss (solid lines) for blown films of samples H and L.

This table indicates that sample H is higher in total and external hazes than sample L if comparison is made at the same shearing level, whereas sample L is higher in internal haze than sample H. This finding possibly arises from the higher crystallinity of sample L as being estimated from a density of 0.924 for sample L against 0.917 for sample H.

The percentage of external haze to total haze is larger than that of the internal haze for both sample H and L. This is especially marked in sample H. The plots of the relative external haze and the relative gloss against pass frequency through the extruder for two samples are shown in Figure 9. Also, the change in transparency of the brown films for these samples is photographically shown in Figure 10.

Figures 8 and 9 and Table III clearly demonstrate that the extent of the surface roughness and the effect of the shearing on the surface roughness are also more marked in sample H, with a higher long-chain branching level, than in sample L, with a lower one.

As is mentioned above, though there is no appreciable difference in the polymer structure of these samples, trace amounts of wax-like materials are possibly produced during the processing. So, for the purpose of investigating the effect of it on the haze and on the gloss of the blown film of the low-density polyethylene, we measured the change in optical properties of a blown film of a commercial low-density polyethylene (melt flow index 5, density 0.924) when it is blended with 1% of a wax which is obtained as a by-product of low-density polyethylene manufacture. This additional experiment resulted in 6.5% of total haze and 11.0% of the gloss for both the base and the blend with 1% wax. We can see, there-
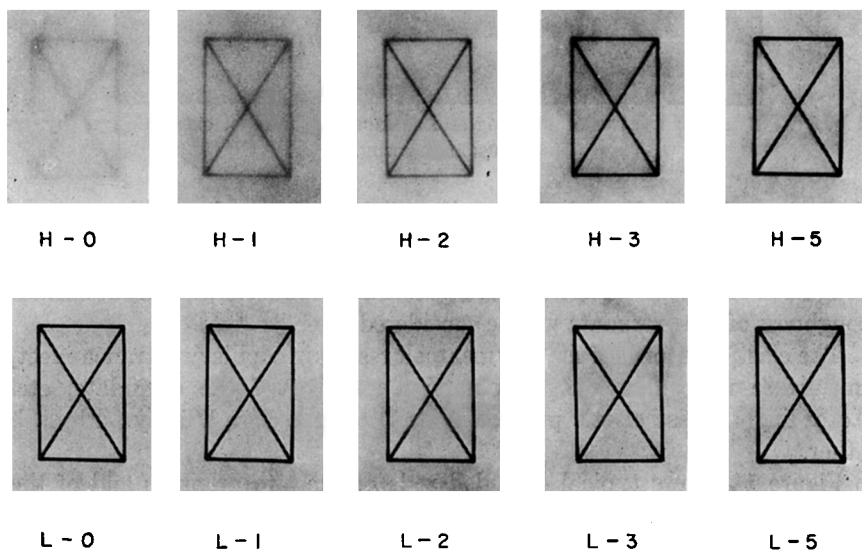

Fig. 10. Variation in transparency of blown film of samples H and L by extrusion shearing (refer to Fig. 9).
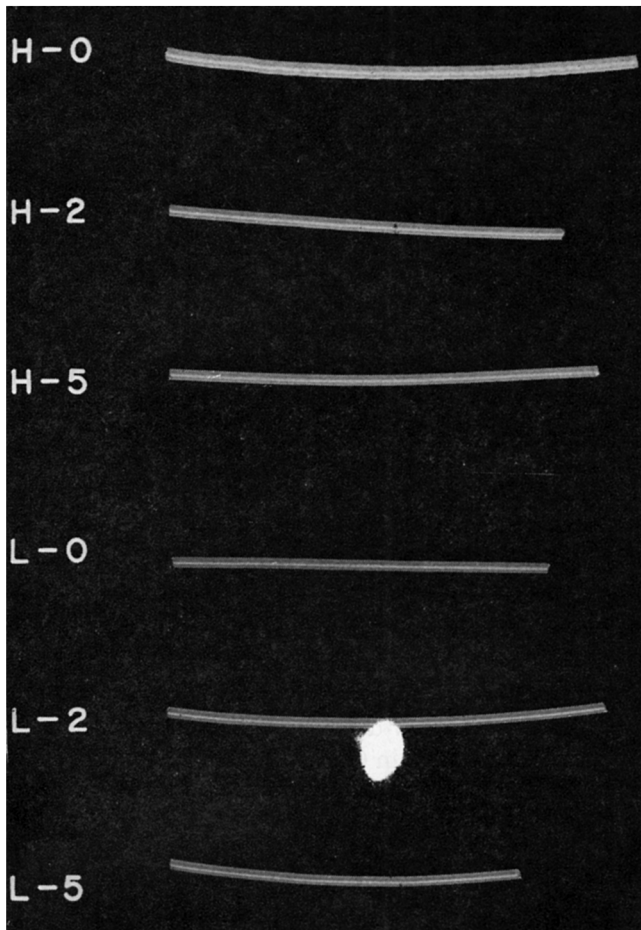
Fig. 11. Variation in extrusion swelling and surface roughness of extruded rods by extrusion shearing.

fore, from this finding that even if a slight amount of wax-like material was produced during the processing of the extrusion, it does not appreciably affect the optical properties of the blown film, that is, the surface roughness of the extrudate.   The mechanism of the formation of the surface roughness of the extrudate will be considered later.

The elastic response of the polymer melt results in capillary entrance effect, in surface roughness, and in extrusion swelling of the extrudate, etc. Accordingly, these elastic properties must have a close affinity with each other.

Figure 11 shows typical extruded rods of the two originals and of the sheared samples after two and five passes through the extruder.   As can be clearly seen from this picture, remarkable surface roughness appears in the extruded rod of sample H-0, of which the extrusion swelling is very large. As the extrusion swelling of the extrudate decreases, however, the degree of
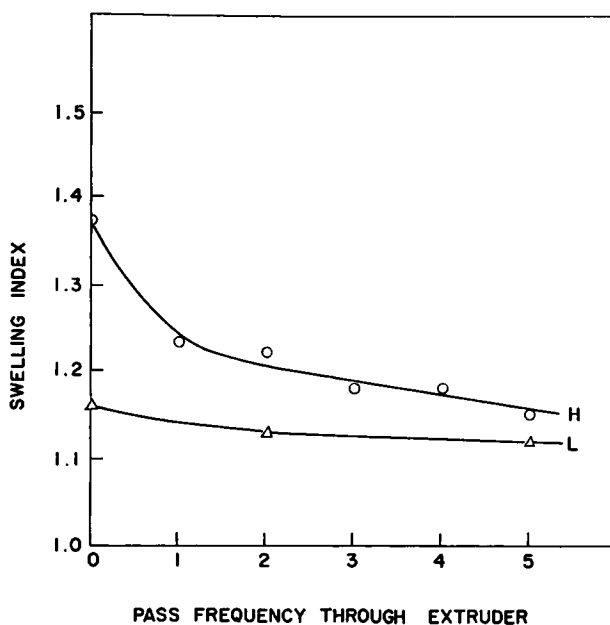
Fig. 12.   Effect of extrusion shearing on extrusion swelling of extrudates.

the surface roughness decreases, too.   The shearing reduces the extrusion swelling of the extrudate of both samples H and L, but the reducing is more notable in sample H than in sample L.

The most striking characteristic found in this measurement is that, despite the impressive difference in the swelling index between two originals, H-0 and L-0, the swelling index of sample H gets nearer to that of sample L with increase in the extent of shearing.   This is illustrated graphically in Figure 12.   Figures 10 and 11 indicate that there is a close affinity between the extrusion swelling and the surface roughness of the extrudate.

DISCUSSION

A common finding in this study is that the shearing affects the viscoelastic properties in the molten state more for the highly branched sample H (with the considerable higher molecular weight species) than for the less branched sample L (with the bell-type molecular weight distribution). For this there are two reasonable explanations: (1) change in the primary structure of the polymers, such as molecular weight, the degree of branching, etc., during the process of extrusion shearing, parameters which are closely associated with the synthesis condition; and/or (2) change in a certain secondary structure, which is the origin of the heterogeneity, that possibly arises from a certain intermolecular interaction depending upon the primary structure of the polymer.

Intrinsic viscometry, gel permeation chromatography, and infrared spectroscopy of the samples of various shearing level, however, indicate no

appreciable variation in the primary structure during the process of extru-
sion shearing. Therefore, the latter explanation will give a special signifi-
cance in causing the distinctive viscoelastic behavior of the long-chain
branched polyethylene melts.

Since the polyethylene has neither polar groups nor oxygen and nitrogen
atoms which have higher electronegativity, it has no energetic intermolec-
ular interactions such as dipole–dipole interaction or interaction due to the
mode of hydrogen bonds. Furthermore, the energetic forces may be
generally broken by the violent thermal molecular motions of the polymer
chains in the molten state. Therefore, in polyethylene melts, intermolec-
ular entanglement should be considered rather than energetic interactions,
based on reasonable mechanical intermolecular interaction.

Two types of entangled network are considered for the long-chain
branched polymer: one arises from looping and coiling of the main chain at
the branching point, and another is generated by intermeshing of the long-
chain branching. Here, we will designate the former as long-range en-
tanglement (LRE) and the latter as short-range entanglement (SRE),
terminology used by McCord and Maxwell.[13]

Generally, the long-chain branched polymer probably requires a long
time for the formation of LRE because of the higher density of polymer
segment, being closely associated with the smaller size of the branched
molecule, and also because of the steric hindrance arising from the presence
of long-chain branching. Formation and disentanglement of LRE may
both take place comparatively easily either in a concentrated polymer
solution or in the molten state of higher temperatures because of the violent
thermal molecular motion of the polymer chain.

If we made an assumption that the probability of the formation of LRE,
P_f, is larger than that of the disentanglement of LRE, P_d, and also that the
LRE is generated during the diffusion of polymer molecules due to
the thermal molecular motion when a polymer molecule frees itself from the
shearing force and, moreover, the length and frequency of long-chain
branching are longer and higher than a certain critical value, then the
density of the LRE will be going up until the equilibrium state obtains.
The polydispersity of molecular weight is especially important when the
polymer has a large amount of long-chain branching. Many studies[25–30]
on the characterization of long-chain branching for low-density poly-
ethylene indicate that the number of long-chain branching increases with
increase in molecular weight, and also its frequency changes depending
upon molecular weight. In such a case it is predicted that LRE does not
form uniformly, but rather, molecular coagulations will result from the
mutual meeting of the molecules having such a long-chain branching as
the value of its length and frequency is higher than the critical value when
$P_f > P_d$. Such a coagulation will behave as the secondary structure from
a structual point of view and will act as the origin of heterogeneity and also
as an elastic flow unit[31,32] from a phenomenologic point of view. In such a
sense we will call it the secondary heterogeneous structure.

Another mechanism of the formation of the secondary heterogeneous structure is reasonably interpreted in terms of phase separation which may be mainly caused by the difference in branching structure between lower and higher molecular weight species. Free energy of a branched polymer system with a molecular weight distribution increases by the additional surface energy due to newly formed phase surface when the coagulation formed as a result of phase separation is subdivided during shear processing. In such a case, the total free energy of a sheared system should be reduced by decreasing phase surface area through recoagulation, that is, shear processing makes a branched polymer system instable, but the system is naturally stabilized by recoagulation of the subdivided coagulation formation of the secondary heterogeneous structure.

It is supposed that the secondary heterogeneous structure will essentially form during the manufacturing process of low-density polyethylene on its way from the reactor to the ethylene gas separator in which the polyethylene is partly dissolved and partly swelled in the pseudoliquid phase of the ethylene under high temperature and high pressure.

A recent study[33] on such a reversibility of the melt flow rate, as pointed out by Prichard and Wissbrun,[10] shows that the increased melt flow indices of the sheared samples H-5 and L-5 reverse to values slightly lower than those of the original samples, H-0 and L-0, when dissolving H-5 and L-5 in hot xylene and subsequently removing the solvent by evaporating under hot nitrogen atmosphere. Also, the reversibility of melt flow rate is obtained by maintaining the sheared sample in the molten state for several hours. This process simulates the manufacturing process of low-density polyethylene, where the reason for the reversed melt flow indices becoming lower than the melt flow indices of the original samples can be ascribed to the shear history of the original samples owing to pelletizing. This finding demonstrates that the possibility of the formation of the secondary heterogeneous structure is present in the manufacturing process of low-density polyethylene and also seems to validate our assumption described above.

If the material has the secondary heterogeneous structure, it significantly affects melt flow behavior and similarly the surface roughness and the extrusion swelling of the extrudate. The relaxation time, τ_l, of the relaxation process due to the disentanglement of the LRE arising from applying shearing force must be much longer than that of the SRE, τ_s, because of higher resistance of the disentanglement of the LRE. Therefore, if the transit time of the polymer melt through the capillary is shorter than τ_l, then the elastic energy for the deformation or for the orientation of the molecular coagulation, i.e., the secondary heterogeneous structure, during transit into the capillary should be largely stored in the system. And to release the stored elastic energy at the outlet of the capillary may cause surface roughness and may increase extrusion swelling of the extrudate. Accordingly, it is considered that the reason why both surface roughness and extrusior swelling of the extrudate of sample H-0 are more pronounced than

those of sample L-0, is that a larger amount of the secondary heterogeneous structure is present in sample H-0 than in sample L-0 (refer to Fig. 11).

It is also supposed that the improvement in transparency of the blown film of low-density polyethylene by water quenching is mainly caused by reducing the surface roughness, being attributed to the fact that the stored elastic energy of the secondary heterogeneous structure is not released by the water quenching but is settled in the film, rather than by reducing of the internal haze. Here it should also be noted that the external haze mainly controls the apparent (total) haze of the blown film, as shown in Table III, i.e., the influence of the internal haze is negligibly small compared with the external haze.

Another point in question is that the internal haze of the film used in this study decreases with increase in the shearing level. This result is allowed to suggest a lowering of the crystallinity during the process of extrusion shearing, but the differential scanning calorimeter study (performed with a Perkin-Elmer DSC-1B, using a heating rate of 20°C/min and 10-mg samples) of the sheared and original unannealed blown film samples unexpectedly shows the opposite result: the value of heat of fusion for the original samples, H-0 and L-0, are 22.1 and 27.3 cal/g, respectively, whereas those for the sheared samples, H-5 and L-5, are 23.4 and 27.7 cal/g, respectively, where the unannealed densities, measured in accordance with ASTM D1505-63T, of these blown film samples, H-0 and H-5, are 0.9178 and 0.9172, respectively, and those of L-0 and L-5 are both 0.9227.

These calorimetric data indicate that the crystallinities of the sheared samples are slightly higher than those of the original samples, but the unannealed density of H-5 is slightly lower than that of H-0, which shows a contradiction when comparing the density with the calorimetric data. The cause of this paradox is not clear within the experimental data of this work, but a change in the crystallinity during the process of extrusion shearing may be considered to be small compared with a change in the internal haze.

It is suggested, consequently, that the decreased internal haze of the sheared samples can also be attributed to the disappearance or change in the form of the secondary heterogeneous structure being involved during the process of extrusion shearing and that the presence of the secondary heterogeneous structure lessens the heat of fusion but increases the internal haze of the extrudate.

When polymeric material has a uniform molecular weight and, moreover, has long-chain branching the length of which is longer than the critical value, the dimensions of the secondary heterogeneous structure possibly grow up on a large scale. Then it is expected that the Newtonian melt viscosity of the material becomes higher than that of a linear polymer with an equivalent molecular weight because of the geometric effect of the secondary heterogeneous structure on the steady-shear viscous flow. Some examples of such a case have been reported for branched polybutadiene[5] and poly(vinyl acetate).[4]

Because of larger capillary end corrections of the original sample H-0 (see Fig. 8), one would expect a large melt elasticity as compared with the sheared sample H-5; and, therefore, the melt viscosity of the original becomes higher than that of the sheared one. However, contrary to expectation, there is no significant difference in their melt viscosities after the capillary end corrections have been made. This finding seems to be ascribed to the fact that the geometric effect of the secondary heterogeneous structure on the steady-shear viscous flow is negligibly small in these polydisperse systems.

In conclusion, the present study suggests that the secondary heterogeneous structure arises in the long-chain branched polymer through phase separation or from the heterogeneous formation of a strongly entangled network at the branching point of long-chain branching in the molten state or in the concentrated solution system, or in the manufacturing process of the low-density polyethylene, and that its presence causes the distinctive viscoelastic properties of the long-chain branched polymer melt. It is believed that the remarkable heterogeneity of sample H-0 is due to a large amount of secondary heterogeneous structure.

References

1. C. A. Sperati, W. A. Franta, and H. W. Starkweather, Jr., *J. Amer. Chem. Soc.*, **75**, 6127 (1953).

2. H. D. Anspon, *Manufacture of Plastics*, Vol. I, W. M. Smith, Ed., Reinhold, New York, 1964, p. 72.

3. H. V. Boenig, *Polyolefins*, Elsevier, Amsterdam, 1966, p. 279.

4. V. C. Long, G. C. Berry, and L. M. Hobbs, *Polymer*, **5**, 517 (1964).

5. G. Kraus and J. T. Gruver, *J. Polym. Sci.*, **3**, 105 (1965).

6. J. E. Guillet, R. L. Combs, D. F. Slonaker, D. A. Weemes, and H. W. Coover, Jr., *J. Appl. Polym. Sci.*, **9**, 767 (1965).

7. R. L. Combs, D. F. Slonaker, and H. W. Coover, Jr., *J. Appl. Polym. Sci.*, **13**, 519 (1969).

8. L. H. Tung, *J. Polym. Sci.*, **46**, 409 (1960).

9. H. P. Schreiber and E. B. Bagley, *J. Polym. Sci.*, **58**, 29 (1962).

10. J. H. Prichard and K. F. Wissbrun, *J. Appl. Polym. Sci.*, **13**, 233 (1969).

11. M. L. Miller, *The Structure of Polymers*, Reinhold, New York, 1966, 122.

12. E. R. Howells and J. J. Benbow, *Trans. J. Plast. Inst.*, **30**, 240 (1962).

13. R. A. McCord and B. Maxwell, *Modern Plastics*, **38** (9), 116 (1961).

14. M. Nagasawa and T. Fujimoto, paper presented at the Sectional Meeting of Autumn of Physical Society of Japan, Nagoya, 1969.

15. L. Wild and R. Guliana, *J. Polym. Sci. A-2*, **5**, 1087 (1967).

16. T. Arai, *A Guide to the Testing of Rheological Properties with Koka Flow Tester*, Maruzen, Tokyo, 1958.

17. J. Brandrup and E. H. Immergut, Eds., *Polymer Handbook*, Interscience, New York, 1966, p. VI-45.

18. E. B. Bagley, *J. Appl. Phys.*, **28**, 624 (1957).

19. J. P. Tordella, *J. Appl. Polym. Sci.*, **7**, 215 (1963).

20. J. J. Benbow and S. Lamb, *SPE Trans. B3*, 7 (1963).

21. J. P. Tordella, *Trans. Soc. Rheol.*, **1**, 203 (1957).

22. E. B. Bagley and A. M. Birks, *J. Appl. Phys.*, **31**, 556 (1960).

23. E. B. Bagley, *J. Appl. Phys.*, **31**, 1126 (1960).

24. T. Fujiki, M. Uemura, and Y. Kosaka, *J. Appl. Polym. Sci.*, **12**, 267 (1968).

25. Q. A. Trementozzi, *J. Polym. Sci.*, **23**, 887 (1957).

26. R. A. Mendelson, *J. Polym. Sci.*, **46**, 493 (1960).

27. J. E. Guillet, *J. Polym. Sci. A*, **1**, 2869 (1963).

28. T. Hama and K. Yamaguchi, paper presented at the 18th Annual Symposium on Polymer Chemistry, Kyoto, Japan, May 1969.

29. W. R. A. D. Moore and W. Millns, *Brit. Polym. J.*, **1**, 81 (1969).

30. T. Takagi, T. Hashimoto, K. Tanaka, and Y. Koya, *Sci. Rept. Toyo Soda Mfg. Co.*, **13**, 126 (1969).

31. M. Mooney and W. E. Wolstenholme, *J. Appl. Phys.*, **25**, 1098 (1954).

32. W. F. Busse, *J. Polym. Sci. A-2*, **5**, 1261 (1967).

33. N. Emura, M. Uemura, and Y. Kosaka, *Jap. Plastics*, **21** (4), 50 (1970).